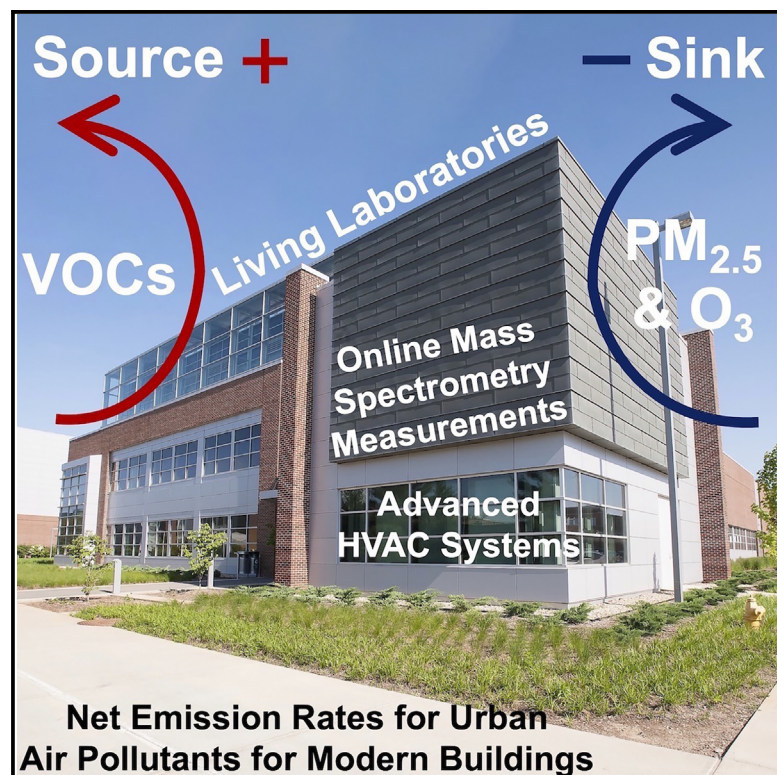


# Modern buildings act as a dynamic source and sink for urban air pollutants

## Graphical abstract



## Authors

Tianren Wu, Antonios Tasoglou, Danielle N. Wagner, ..., Philip S. Stevens, Nusrat Jung, Brandon E. Boor

## Correspondence

wutr@ucmail.uc.edu (T.W.),  
bboor@purdue.edu (B.E.B.)

## In brief

Wu et al. present real-time direct measurements of urban air pollutant exchange between an advanced ventilation system of a high-performance LEED-certified building and outdoor air. This work demonstrates that modern buildings are a dynamic emission source of climate- and health-relevant volatile chemicals to urban atmospheric environments.

## Highlights

- Modern buildings continually release volatile chemicals into the outdoor atmosphere
- Buildings can be significant emission sources of reactive monoterpenes and siloxanes
- Building source-sink behavior changes with human occupancy and ventilation conditions
- Direct VOC emissions from buildings must be considered in urban air pollution models



## Article

# Modern buildings act as a dynamic source and sink for urban air pollutants

Tianren Wu,<sup>1,\*</sup> Antonios Tasoglou,<sup>2</sup> Danielle N. Wagner,<sup>3,4</sup> Jinglin Jiang,<sup>3,4</sup> Heinz J. Huber,<sup>5</sup> Philip S. Stevens,<sup>6,7</sup> Nusrat Jung,<sup>9</sup> and Brandon E. Boor<sup>3,4,8,\*</sup>

<sup>1</sup>Civil & Architectural Engineering & Construction Management, University of Cincinnati, Cincinnati, OH, USA

<sup>2</sup>RJ Lee Group Inc., Monroeville, PA, USA

<sup>3</sup>Lyles School of Civil Engineering, Purdue University, West Lafayette, IN, USA

<sup>4</sup>Ray W. Herrick Laboratories, Center for High Performance Buildings, Purdue University, West Lafayette, IN, USA

<sup>5</sup>Edelweiss Technology Solutions, LLC, Novelty, OH, USA

<sup>6</sup>O'Neill School of Public & Environmental Affairs, Indiana University, Bloomington, IN, USA

<sup>7</sup>Department of Chemistry, Indiana University, Bloomington, IN, USA

<sup>8</sup>Lead contact

\*Correspondence: [wutr@ucmail.uc.edu](mailto:wutr@ucmail.uc.edu) (T.W.), [bboor@purdue.edu](mailto:bboor@purdue.edu) (B.E.B.)

<https://doi.org/10.1016/j.crsus.2024.100103>

**SCIENCE FOR SOCIETY** Buildings account for a significant fraction of the land area in cities and actively exchange air with their proximate outdoor environments via mechanical ventilation systems. However, the direct impact of buildings on urban air pollution remains poorly characterized. Due to reductions in traffic-associated emissions of volatile organic compounds (VOCs), volatile chemical products, which are widely used inside buildings, have become a major VOC source in urban areas. Indoor-generated VOCs are likely to be an important contributor to the VOC burden of the urban atmosphere, and ventilation systems provide a pathway for VOCs to be released outdoors. Here, we show how modern buildings act as significant emission sources of VOCs for the outdoor environment. Our results demonstrate that future air quality monitoring efforts in cities need to account for direct VOC discharge from buildings in order to capture emerging sources of environmental pollution that can impact the climate and human health.

## SUMMARY

Urban air undergoes transformations as it is actively circulated throughout buildings via ventilation systems. However, the influence of air exchange between outdoor and indoor atmospheres on urban air pollution is not well understood. Here, we quantify how buildings behave as a dynamic source and sink for urban air pollutants via high-resolution online mass spectrometry measurements. During our field campaign in a high-performance office building, we observed that the building continually released volatile organic compounds (VOCs) into the urban air and removed outdoor ozone and fine particulate matter. VOC emissions from people, their activities, and surface reservoirs result in significant VOC discharge from the building to the outdoors. Per unit area, building emissions of VOCs are comparable to traffic, industrial, and biogenic emissions. The building source-sink behavior changed dynamically with occupancy and ventilation conditions. Our results demonstrate that buildings can directly influence urban air quality due to substantial outdoor-indoor air exchange.

## INTRODUCTION

A fundamental understanding of the fate and transport of urban air pollutants is important for developing mitigation strategies and policies that can improve urban air quality and reduce adverse impacts on human health and the climate. Numerous studies have demonstrated the significant impact of traffic, industrial, and biogenic emissions on urban air pollution.<sup>1–5</sup> However, the influence of urban air pollutant interactions with build-

ings has often been overlooked. Buildings account for a great fraction of the land area in cities and provide a significant amount of occupied indoor space. To meet building ventilation and thermal comfort requirements, a substantial amount of air is actively exchanged between a building and its proximate urban atmosphere. This dynamic air exchange may have important implications for urban air quality due to both indoor-to-outdoor and outdoor-to-indoor transport and transformations of pollutants, especially in densely populated megacities.<sup>6–11</sup>



Modern public and commercial buildings are typically equipped with heating, ventilation, and air conditioning (HVAC) systems to provide improved indoor air quality and thermal comfort. HVAC systems serve as an interface to exchange indoor and outdoor air; this provides a dynamic pathway for buildings to impact urban air quality. When urban air is mechanically circulated throughout buildings, its composition may significantly change due to interactions with HVAC components, indoor air, occupants, and indoor surfaces. For example, air filters installed in the HVAC system can remove outdoor particles in the incoming air with size-dependent efficiency.<sup>12</sup> Heating elements can result in the loss of semi-volatile content in the particle phase.<sup>13</sup> Indoor surfaces can remove ozone (O<sub>3</sub>) due to their enhanced O<sub>3</sub> reactivity.<sup>14</sup> Conversely, building materials, interior furnishings, human metabolism, and occupant activities, such as cooking, cleaning and disinfecting surfaces, and use of volatile chemical products (VCPs), can release a variety of gaseous and particulate contaminants,<sup>15–21</sup> which may be directly exhausted into the urban atmosphere via the HVAC system.

Pollutant emissions from indoor sources can affect ambient air quality. The mixing ratios of volatile organic compounds (VOCs) in indoor air are typically 2 to 10 times higher than outdoors<sup>22,23</sup> and indoor VOC emissions can contribute to urban VOC concentrations via building ventilation.<sup>11,24</sup> Sheu et al. demonstrated the indoor-to-outdoor transport of a series of VOCs emitted from long-lived indoor surface reservoirs in an unoccupied residential house during simulated natural ventilation experiments.<sup>10</sup> Furthermore, recent studies have indicated that due to declining VOC emissions from traffic, the use of VCPs has become a major contributor to VOCs in urban areas.<sup>25</sup> Much of the use of VCPs, such as consumer and personal care products (PCPs), occurs in occupied indoor environments.<sup>19,24,26</sup>

VOCs released from indoor use of VCPs can be transported outdoors to the urban atmosphere via mechanical/natural ventilation and exfiltration. This was partially reflected by consistent observations of tracer compounds of consumer products in both urban and indoor measurements. Measurements in a university classroom, athletic center, and residential homes indicate that volatile methyl siloxanes, a group of compounds widely used in PCPs, constitute a large fraction of total indoor VOC mass concentrations,<sup>22,26–29</sup> while urban outdoor air measurements show abundant levels of decamethylcyclopentasiloxane (siloxane D5) that correlate with population density.<sup>9,25</sup> This indicates that a fraction of urban VOCs can originate from indoor VCP use.

Indoor-to-outdoor transport of indoor-generated VOCs and the transformation of outdoor air pollutants, such as O<sub>3</sub> and fine particulate matter (PM<sub>2.5</sub>), upon their delivery to indoor spaces are likely to be strongly influenced by characteristics of the indoor environment,<sup>30–32</sup> human occupancy,<sup>33,34</sup> and the operational conditions of the HVAC system.<sup>35</sup> The latter is often dynamically changing over various timescales, from minutes to weeks, due to building automation system control logic according to indoor and outdoor environmental conditions and energy use patterns, among other factors. To comprehensively understand the impact of buildings on urban air quality, direct air pollutant measurements from HVAC systems are needed to investigate the dynamic exchange of gaseous and particulate

contaminants between indoor and outdoor spaces and the factors that affect such exchanges.

To fill this important knowledge gap, we investigated the source and sink effects of a mechanically ventilated, realistic, open-plan office and its HVAC system on urban air pollutants through a comprehensive 1-month measurement campaign during the heating season. The office is located in a high-performance, Leadership in Energy and Environmental Design (LEED) Gold-certified building in central Indiana, US. The office is continuously mechanically ventilated by an independent air handling unit (AHU) (Figure S1). There is a minimum efficiency reporting value (MERV) 8 pre-filter and a MERV 14 final-filter in the AHU to remove particles in the supply air. The supply air contains a mixture of outdoor air and recirculated return air, and the supply air exchange rate was maintained at  $\sim 7 \text{ h}^{-1}$ . The field measurement campaign was performed during the heating season, and the HVAC system was operated under the normal automation mode for 23 days and 2 days under an override automation mode. The normal mode is based upon mixed air temperature control, whereby the system dynamically adjusts the fraction of recirculated return air and outdoor air in the supply air to maintain the mixed air temperature at the setpoint. The mixed air temperature setpoints were 8.8°C and 17.2°C, pre-determined by the building design engineer (Figure S2). The normal mode represents a common HVAC system operation strategy in modern, mechanically ventilated buildings in the US. Under the override mode, the supply air only contained outdoor air to simulate buildings with a single-pass ventilation system.

Three types of common urban air pollutants were examined in this study, including VOCs, O<sub>3</sub>, and PM<sub>2.5</sub>. Direct, spatiotemporally resolved measurements of VOCs, O<sub>3</sub>, and PM<sub>2.5</sub> and mechanical ventilation conditions were performed to quantify net mass emission rates from the office and its HVAC system to the urban atmosphere. VOCs were monitored in real-time with a high-resolution proton transfer reaction time-of-flight mass spectrometer (PTR-TOF-MS) using hydronium (H<sub>3</sub>O<sup>+</sup>) as the reagent ion (henceforth, each VOC is referred to as VOC<sub>PTR</sub>). The net mass emission rate was calculated as the product of the exhaust volumetric airflow rate and the pollutant concentration in the exhaust air minus that of the intake volumetric airflow rate and the outdoor air pollutant concentration.

## RESULTS AND DISCUSSION

The 1-month field measurement campaign revealed that the high-performance building acted as a net sink for O<sub>3</sub> and PM<sub>2.5</sub> (with respect to outdoors) and a net source for VOCs (with respect to outdoors) (Figure 1). The mean net emission rates ( $E_{net}$ ) for the modern office and its HVAC system were  $-47.5 \pm 31.2$ ,  $-2.4 \pm 2.4$ , and  $78.0 \pm 73.5 \text{ mg h}^{-1}$  for O<sub>3</sub>, PM<sub>2.5</sub>, and total VOC<sub>PTR</sub>, respectively. Normalized by the office floor area, the net emission rates were  $-0.457 \pm 0.300$ ,  $-0.023 \pm 0.023$ , and  $0.750 \pm 0.707 \text{ mg h}^{-1} \text{ m}^{-2}$  for O<sub>3</sub>, PM<sub>2.5</sub>, and total VOC<sub>PTR</sub>, respectively. The mean daily human occupancy (24 h average) was 1.54 ( $\pm 2.15$ ) and the mean exhaust (outdoor) volumetric airflow rate was  $728 (\pm 388) \text{ ft}^3 \text{ min}^{-1}$ , equivalent to an outdoor air exchange rate of  $\sim 3.7 \text{ h}^{-1}$ . Henceforth,

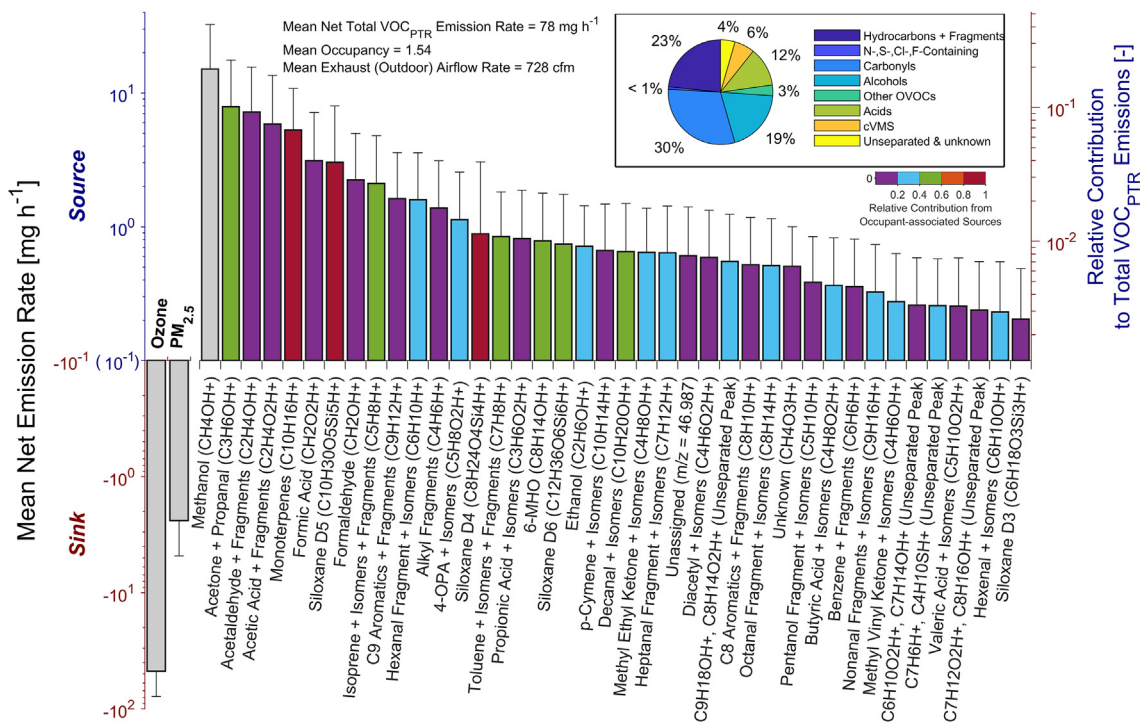


**Figure 1. Net emission rates of urban air pollutants for a modern building**

The mean net emission rates of O<sub>3</sub>, PM<sub>2.5</sub>, and VOCs (40 ions with the highest net emission rates as determined via PTR-TOF-MS measurements in H<sub>3</sub>O<sup>+</sup> mode). The color scheme of the bar plots of VOC<sub>PTR</sub> indicates the relative contribution from occupant-associated sources (details in the supplemental information). The error bars represent the standard deviation. The right axis shows the relative contribution of each VOC<sub>PTR</sub> to the total VOC<sub>PTR</sub> net emission rate. The pie chart indicates the relative contribution of each group of VOC<sub>PTR</sub> to the total VOC<sub>PTR</sub> net emission rate.

$E_{VOC_{PTR}}$ ,  $E_{Ozone}$ , and  $E_{PM_{2.5}}$  are used to refer to the net emission rates for each air pollutant category.

### Building sink effects for outdoor O<sub>3</sub> and PM<sub>2.5</sub>

As the most important indoor oxidant, O<sub>3</sub> exhibits enhanced reactivities with indoor and human surfaces.<sup>36,37</sup> We observed a mean O<sub>3</sub> deposition velocity of  $0.045 \pm 0.0083$  cm s<sup>-1</sup> to indoor surfaces and a deposition velocity of  $1.35 \pm 0.63$  cm s<sup>-1</sup> person<sup>-1</sup> to the human body (assuming a surface area of 1.7 m<sup>2</sup> per person<sup>38</sup>),<sup>39</sup> equivalent to a loss rate of  $\sim 3.4$  h<sup>-1</sup> and  $\sim 0.25$  h<sup>-1</sup> person<sup>-1</sup>, respectively. In addition to the net emission rate, the sink effect for outdoor O<sub>3</sub> as it is transported throughout the office and its HVAC system can be viewed in terms of an effective clean air delivery rate (CADR), a metric used for evaluating indoor air cleaners. The mean CADR of the office and its HVAC system for the urban atmosphere was  $618 (\pm 347)$  m<sup>3</sup> h<sup>-1</sup> for O<sub>3</sub> (CADR<sub>O<sub>3</sub></sub>), equivalent to  $5.94 (\pm 3.34)$  m<sup>3</sup> h<sup>-1</sup> per m<sup>2</sup> office area.

Heterogeneous reactions with indoor surfaces and occupants can effectively remove O<sub>3</sub> and are expected to be the major sink in the office. O<sub>3</sub> can readily react with unsaturated organic compounds in organic films or deposited particles on indoor surfaces, human surfaces, and soiled clothing.<sup>37,40</sup> Indoor measurements of surface samples in a variety of indoor environments at a university indicated that unsaturated organics are ubiquitous on indoor surfaces and concentrations of C=C bonds varied between 0.1–3.9 and 0.06–2.4 μmol

m<sup>-2</sup> on glass and paint, respectively.<sup>41</sup> Human skin continuously produces skin oil, which contains a variety of unsaturated organic compounds in the condensed phase, such as squalene, triglycerides, fatty acids, cholesterol, and others.<sup>42,43</sup> The concentration of C=C bonds in human skin oil is  $\sim 2.9$ – $4.4$  mmol m<sup>-2</sup>, with about half contributed by squalene.<sup>37,42</sup> In addition to surface reactions, O<sub>3</sub> can react with some unsaturated gas-phase VOCs, such as monoterpenes, 6-methyl-5-heptene-2-one (6-MHO), and geranyl acetone. However, due to the low concentrations of these VOCs (on the level of several ppb), we estimated that gas-phase reactions contributed less than 5% toward O<sub>3</sub> loss in the office. In addition, O<sub>3</sub> reactions with NO and NO<sub>2</sub> are likely negligible since the concentration of NO was consistently below 1 ppb (via supplemental measurements with a NO<sub>x</sub> analyzer). There were no obvious indoor O<sub>3</sub> sources in the office, such as photocopiers or air purifiers.<sup>44</sup>

PM<sub>2.5</sub> in the urban atmospheric airflow can be effectively removed when circulated throughout the office and its HVAC system. A two-stage filter setup (MERV 8 + MERV 14) was installed in the AHU to remove PM<sub>2.5</sub> in the supply air; it is expected to be the dominant PM<sub>2.5</sub> removal mechanism. Although particle deposition onto duct and indoor surfaces also occurs, they are considered to contribute less to PM<sub>2.5</sub> removal as compared with continuous air filtration with the MERV 8 + 14 filters.<sup>12,45,46</sup> On the other hand, occupants and their activities can

induce indoor PM<sub>2.5</sub> emissions.<sup>47</sup> Strong indoor PM<sub>2.5</sub> emission sources, such as combustion and cooking, typically do not occur in office buildings.<sup>48,49</sup> The major indoor emission source is likely mechanical processes induced by occupants, such as skin shedding and particle resuspension, which can contribute to indoor PM<sub>10</sub> concentrations,<sup>50</sup> and, to a lesser extent, PM<sub>2.5</sub> concentrations.<sup>51</sup> However, since the office workers remained seated and did not engage in intense physical activity,<sup>52</sup> the indoor PM<sub>2.5</sub> concentration remained at a low level during the campaign. The median indoor PM<sub>2.5</sub> mass concentration was 1.95 μg m<sup>-3</sup> (interquartile range [IQR]: 1.50–2.79 μg m<sup>-3</sup>), with a consistently low indoor-to-outdoor ratio (median: 0.23; IQR: 0.17–0.32). The correlation between indoor PM<sub>2.5</sub> concentrations and occupancy was weak (Pearson's  $r = 0.17$ ), indicating that human emissions might not be a significant source of PM<sub>2.5</sub> in this particular indoor space. In addition, although printers could be a large emitter of indoor PM<sub>2.5</sub>,<sup>53</sup> they were not present in the office.

We estimated the net PM<sub>2.5</sub> removal efficiency of the office and its HVAC system during the campaign to be 74% ± 2% ( $R^2 = 0.91$ ). This was done by applying a linear regression to the PM<sub>2.5</sub> outdoor air intake mass flux and the net PM<sub>2.5</sub> emission rate. Considering that PM<sub>2.5</sub> removal is mainly attributed to the two HVAC filters and there are no significant PM<sub>2.5</sub> emission sources in the office, this value agrees well with the combined PM<sub>2.5</sub> filtration efficiency of the MERV 8 + 14 filters as estimated in a previous study (median: 78%, IQR: 75%–81%).<sup>12</sup> The mean CADR of the office and its HVAC system for PM<sub>2.5</sub> (CADR<sub>PM<sub>2.5</sub></sub>) was 785 (±771) m<sup>3</sup> h<sup>-1</sup> for the urban atmosphere during the campaign, equivalent to 7.55 (±7.41) m<sup>3</sup> h<sup>-1</sup> per m<sup>2</sup> of office area.

### Mechanically ventilated buildings as a significant source of VOCs to urban air

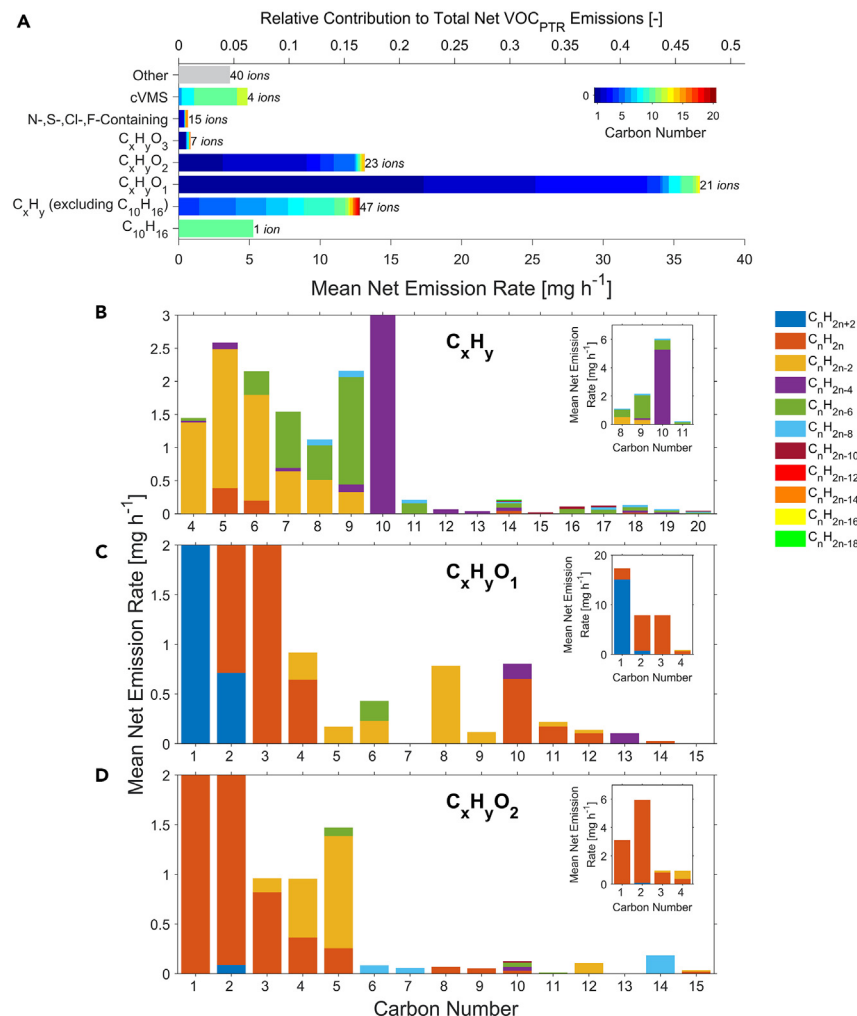
Significant VOC emissions from the office to the urban atmosphere were observed during the campaign. 37.33 g of VOC<sub>PTR</sub> were emitted from the office to the urban atmosphere over 19.93 days with a mean emission rate of 0.75 mg h<sup>-1</sup> per m<sup>2</sup> office area. ~160 product ions detected by the PTR-TOF-MS were included in this study, and we reported the  $E_{VOC_{PTR}}$  for the product ions rather than the species (Table S1). Figure 1 presents the net emission rates of the 40 ions with the highest net emission rates, which contributed 91.4% to the total  $E_{VOC_{PTR}}$ . The office and its HVAC system consistently behaved as a net emission source for nearly all ions, aside from an ion at  $m/z$  116.905 (tentatively CCl<sub>3</sub><sup>+</sup>),<sup>21,22</sup> of which the net emission rate was sometimes positive during occupied periods and negative during unoccupied periods. CH<sub>4</sub>OH<sup>+</sup> (methanol), C<sub>3</sub>H<sub>6</sub>OH<sup>+</sup> (acetone and propanal), C<sub>2</sub>H<sub>4</sub>OH<sup>+</sup> (acetaldehyde and fragments), C<sub>2</sub>H<sub>4</sub>O<sub>2</sub>H<sup>+</sup> (acetic acid and fragments), C<sub>10</sub>H<sub>16</sub>H<sup>+</sup> (monoterpenes), C<sub>10</sub>H<sub>30</sub>O<sub>5</sub>Si<sub>5</sub>H<sup>+</sup> (siloxane D5), and CH<sub>2</sub>O<sub>2</sub>H<sup>+</sup> (formic acid) are the seven compounds with the highest mean net emission rates, contributing 61% to the total  $E_{VOC_{PTR}}$ .

The mean net emission rate of C<sub>10</sub>H<sub>16</sub>H<sup>+</sup> (monoterpenes) was 5.27 (±5.57) mg h<sup>-1</sup> and was 0.051 (±0.054) mg h<sup>-1</sup> m<sup>-2</sup> after normalizing by the office floor area. During high-occupancy periods (10:00–18:00 on weekdays), the normalized value was 0.0648 (±0.257) mg h<sup>-1</sup> m<sup>-2</sup>. The ion is of particular interest since

monoterpenes play a significant role in atmospheric chemistry and the formation of secondary organic aerosol (SOA).<sup>54</sup> In comparison, biogenic emissions of monoterpenes from forests and other vegetation areas can result in net emission fluxes of 0.115–1.22 mg h<sup>-1</sup> m<sup>-2</sup>.<sup>55–59</sup> Considering that office buildings in densely populated megacities often contain offices across multiple stories, the net emission rates of monoterpenes from office buildings per unit urban land area could be comparable to, or even greater, than those from forests and other vegetation areas per unit land area. Coggon et al. reported a monoterpene urban emission flux of 0.613–1.02 mg h<sup>-1</sup> m<sup>-2</sup> from VCPs and other anthropogenic sources in New York City, New York, US, indicating that anthropogenic monoterpene emission fluxes in densely populated regions are comparable to those observed in natural environments.<sup>9</sup>

We determined a mean net emission rate of 0.750 ± 0.707 mg h<sup>-1</sup> per m<sup>2</sup> office area for total VOC<sub>PTR</sub> in this study. By contrast, a VOC emission inventory established for the city of Qingdao, China, in 2016 reported urban VOC emission rates of 0.309, 0.0405, and 0.766 mg h<sup>-1</sup> m<sup>-2</sup> for on-road mobile sources, non-road mobile sources, and industrial processes.<sup>60</sup> Another urban VOC emission inventory showed emission rates of 1.14 and 0.932 mg h<sup>-1</sup> m<sup>-2</sup> for traffic exhaust and industrial processes in the city of Chengdu, China.<sup>61</sup> D'Angiola et al. estimated the emission rate of non-methane VOCs from on-road traffic emissions to be 2.18 mg h<sup>-1</sup> m<sup>-2</sup> in Buenos Aires, Argentina.<sup>62</sup> Kota et al. reported hourly average emission fluxes of 18 VOCs from vehicle exhaust ranging from ~0.3 to 1.1 mg h<sup>-1</sup> m<sup>-2</sup> in an urban residential area of Houston, Texas, US.<sup>63</sup> Measurements in US cities, including New York City boroughs, Chicago, Pittsburgh, and Boulder, showed that mobile sources resulted in VOC emission rates ranging between 0.208 and 20.8 mg h<sup>-1</sup> m<sup>-2</sup>.<sup>8</sup> These results demonstrate that direct VOC emissions from modern buildings via mechanical ventilation systems could be comparable to some of the major VOC sources in urban environments, such as traffic emissions and industrial processes, and need to be considered in air pollution and climate models of urban atmospheric environments.

A recent study reported indoor-to-outdoor VOC emission rates from an unoccupied, single-family home under simulated natural ventilation conditions.<sup>10</sup> A comparison of the emission rates of selected VOCs is shown in Table S2. Despite differences in building type, ventilation system, and occupancy, the emission rates of selected VOCs generally show good agreement with differences less than a factor of 4. For example, the mean net emission rate of monoterpenes (C<sub>10</sub>H<sub>16</sub>H<sup>+</sup>) per unit office area was 0.0501 mg h<sup>-1</sup> m<sup>-2</sup>, while the sum of average indoor-to-outdoor emission rates of  $\alpha$ -pinene,  $\beta$ -pinene, and limonene was 0.0432 mg h<sup>-1</sup> m<sup>-2</sup> in the residential house. However, Sheu et al.<sup>10</sup> observed the largest VOC emissions for furfural with an average rate of 0.743 mg h<sup>-1</sup> m<sup>-2</sup>, while the mean net emission rate of C<sub>5</sub>H<sub>4</sub>O<sub>2</sub>H<sup>+</sup> (furfural + isomers) in this study was only 8.40 × 10<sup>-4</sup> mg h<sup>-1</sup> m<sup>-2</sup>. This can be attributed to the wood frame structure of the home, resulting in significant furfural emissions from wood decomposition,<sup>28</sup> while this study site is within a high-performance building with a reinforced concrete structure with some wooden materials.



The detected ions were separated into different groups according to their chemical formula, including hydrocarbons and fragments (C<sub>x</sub>H<sub>y</sub>H<sup>+</sup>), oxygenated VOCs (OVOCs) with one, two, or three oxygen atoms (C<sub>x</sub>H<sub>y</sub>O<sub>1</sub>H<sup>+</sup>, C<sub>x</sub>H<sub>y</sub>O<sub>2</sub>H<sup>+</sup>, C<sub>x</sub>H<sub>y</sub>O<sub>3</sub>H<sup>+</sup>), cyclic volatile methyl siloxanes (cVMSs), and N-, S-, Cl-, and F-containing compounds (Figure 2). Significant indoor-to-outdoor emissions of OVOCs were observed, which can contribute to urban total OVOC emissions.<sup>64</sup> On average, C<sub>x</sub>H<sub>y</sub>O<sub>1</sub>H<sup>+</sup> accounted for most of the total E<sub>VOC<sub>PTR</sub></sub> (47.2%), followed by C<sub>x</sub>H<sub>y</sub>H<sup>+</sup> and C<sub>x</sub>H<sub>y</sub>O<sub>2</sub>H<sup>+</sup>, accounting for 23.2% and 16.9% of the total E<sub>VOC<sub>PTR</sub></sub>, respectively. The mean net emission rates of C<sub>x</sub>H<sub>y</sub>H<sup>+</sup>, C<sub>x</sub>H<sub>y</sub>O<sub>1</sub>H<sup>+</sup>, and C<sub>x</sub>H<sub>y</sub>O<sub>2</sub>H<sup>+</sup> ions were then categorized by carbon number and the pattern in the number of carbon and hydrogen atoms (Figures 2, S11, and S12). C<sub>4</sub> to C<sub>10</sub> ions dominate in the emission of C<sub>x</sub>H<sub>y</sub>H<sup>+</sup> ions, with a significant contribution from C<sub>10</sub>H<sub>16</sub>H<sup>+</sup> (monoterpenes; Figure 2B). In addition, contributions from C<sub>n</sub>H<sub>2n</sub>H<sup>+</sup> and C<sub>n</sub>H<sub>2n-6</sub>H<sup>+</sup> ions were also observed. The emissions of OVOCs C<sub>x</sub>H<sub>y</sub>O<sub>1</sub>H<sup>+</sup> and C<sub>x</sub>H<sub>y</sub>O<sub>2</sub>H<sup>+</sup> were mainly attributed to C<sub>1</sub> to C<sub>4</sub> ions and C<sub>1</sub> to C<sub>5</sub> ions, respectively. C<sub>n</sub>H<sub>2n+2</sub>O<sub>1</sub>H<sup>+</sup> and C<sub>n</sub>H<sub>2n</sub>O<sub>1</sub>H<sup>+</sup> dominated the emissions of C<sub>x</sub>H<sub>y</sub>O<sub>1</sub>H<sup>+</sup> ions, while C<sub>n</sub>H<sub>2n</sub>O<sub>2</sub>H<sup>+</sup> dominated in the emission of C<sub>x</sub>H<sub>y</sub>O<sub>2</sub>H<sup>+</sup> ions.

**Figure 2. Categorization of VOC net emission rates**

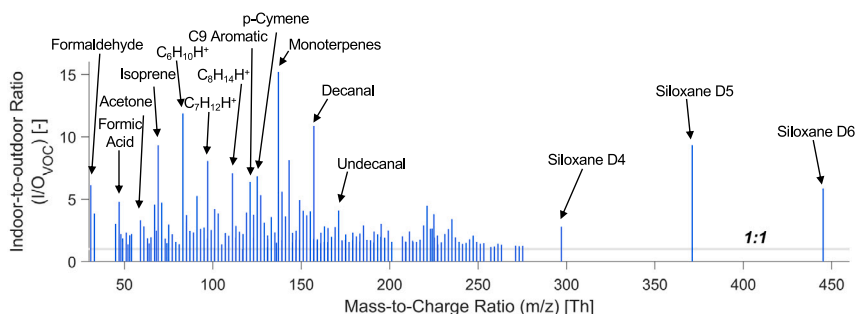
The mean net emission rate of (A) VOC<sub>PTR</sub> grouped by chemical formula, including hydrocarbons and fragments (C<sub>x</sub>H<sub>y</sub>H<sup>+</sup>); oxygenated VOCs (OVOCs) with one, two, or three oxygen atoms (C<sub>x</sub>H<sub>y</sub>O<sub>1</sub>H<sup>+</sup>, C<sub>x</sub>H<sub>y</sub>O<sub>2</sub>H<sup>+</sup>, and C<sub>x</sub>H<sub>y</sub>O<sub>3</sub>H<sup>+</sup>); cVMSs; and N-, S-, Cl-, and F-containing compounds and (B–D) VOC<sub>PTR</sub> grouped by the number of carbon and oxygen atoms. Given the importance of C<sub>10</sub>H<sub>16</sub>H<sup>+</sup> in atmospheric chemistry and its utility as a marker for anthropogenic monoterpenes in urban areas, it was separated from the C<sub>x</sub>H<sub>y</sub>H<sup>+</sup> category in (A).

Figure S7 is a mass defect plot that shows the net emission rates of isobaric compounds in the lower mass range. Emissions for several types of ions were clearly observed, such as C<sub>n</sub>H<sub>2n-2</sub>H<sup>+</sup>, C<sub>n</sub>H<sub>2n</sub>OH<sup>+</sup>, C<sub>n</sub>H<sub>2n</sub>H<sup>+</sup>, and C<sub>n</sub>H<sub>2n-2</sub>OH<sup>+</sup>. Among these types, the ions in the form of C<sub>n</sub>H<sub>2n</sub>OH<sup>+</sup> accounted for 24.3% of the total E<sub>VOC<sub>PTR</sub></sub>. Following that, the ions with the form of C<sub>n</sub>H<sub>2n</sub>O<sub>2</sub>H<sup>+</sup> contribute 13.6%, which are associated with acids, hydroxyl carbonyls, and esters.

The OVOCs were further divided into alcohols, acids, carbonyls, and other OVOCs based on information from previous indoor air studies with PTR-TOF-MS.<sup>26–28,32</sup> We found that, on average, carbonyl compounds contributed the most to the total E<sub>VOC<sub>PTR</sub></sub> (30%; Figure 1, pie chart), followed by hydrocarbons and fragments (23%), alcohols (19%), acids (12%), and cVMSs (6%). Previous measurements indicated that carbonyl compounds can be emitted from a variety of indoor sources, such as human breath and skin, PCPs, building materials, and O<sub>3</sub> reactions with human skin lipids and indoor surfaces.<sup>21,27,36,65</sup>

Caution needs to be taken when interpreting the relative fractions of emissions from different categories. Due to the fragmentation in the PTR-TOF-MS, some OVOCs (e.g., aldehydes, alcohols) may fragment into C<sub>x</sub>H<sub>y</sub>H<sup>+</sup> ions,<sup>66</sup> which could be categorized as hydrocarbons.

The indoor-to-outdoor ratios of the VOC<sub>PTR</sub> concentrations were consistently high for the high-performance building (mean: 2.70 ± 1.39; based on volumetric mixing ratios; Figure 3). Positive matrix factorization (PMF; details in the supplemental information) analysis indicated that over a 24 h period, office workers and their activities contributed more than 34% to the total office VOC<sub>PTR</sub>, while during the high-occupancy hours (10:00–18:00 on weekdays), they contributed more than 43%. Human-related indoor VOC emissions have been investigated in many studies. Human metabolism results in the emissions of several hundred bioeffluent VOCs through exhaled breath and skin.<sup>67</sup> The dominant VOCs include compounds such as acetone, isoprene, methanol, ethanol, acetaldehyde, formic



**Figure 3. Indoor-to-outdoor ratios of VOCs during the measurement campaign**

Mean indoor-to-outdoor ratios of VOC<sub>PTR</sub> concentrations as a function of mass-to-charge ratio as detected by the PTR-TOF-MS in H<sub>3</sub>O<sup>+</sup> mode. Indoor VOC mixing ratios were measured in the return air duct at around 1.2 m downstream of the return air grille.

acid, and acetic acid.<sup>67,68</sup> Heterogeneous reactions between unsaturated organic compounds in human skin oil and O<sub>3</sub> also produce a wide range of carbonyl VOCs, such as acetone, decanal, 4-oxopentanal (4-OPA), and 6-MHO.<sup>21,36,37,39</sup>

Indoor application of leave-on PCPs (e.g., deodorants, perfumes, lotions, hair care products) on the human body can cause off-gassing of the contained volatile compounds, such as cVMSs (e.g., siloxane D5), monoterpenes, alcohols, hexanal, and glycols, from human surfaces to indoor air.<sup>6,8,20,24–27</sup> cVMS emissions have received growing attention in recent years since they are one of the signature compounds of VCPs, which have been found to contribute significantly to the atmospheric VOC burden in industrialized cities and have a relatively long atmospheric lifetime.<sup>6,8,25</sup> During the campaign, the average net emission rate of siloxane D5 to the atmosphere was  $3.03 \pm 4.95 \text{ mg h}^{-1}$  ( $29.1 \pm 47.6 \mu\text{g h}^{-1}$  per m<sup>2</sup> office area). In comparison, previous measurements in an urban area in central Europe indicated a median emission flux of  $6 \mu\text{g h}^{-1}$  per m<sup>2</sup> urban area for D5.<sup>64</sup> In this study, the sum of cVMS net emission rates (siloxane D3, D4, D5, and D6) was  $4.86 \pm 5.50 \text{ mg h}^{-1}$ , which accounts for 6.23% of the total  $E_{\text{VOC}_{\text{PTR}}}$ . Given that the average occupancy was 1.54 (24 h average) and assuming that the emission of cVMSs was only from the office workers (validated by the PMF analysis), the average per-person emission rates of siloxane D5 and the sum of cVMSs were  $1.97 \pm 3.21$  and  $3.16 \pm 3.57 \text{ mg h}^{-1} \text{ person}^{-1}$  (assuming no loss due to deposition and reactions inside the office and its HVAC system), which agree well with previously reported values of 0.36–9.8 and  $2.8 \text{ mg h}^{-1} \text{ person}^{-1}$ , respectively, in a university classroom.<sup>21,26</sup> The per-person emission rate of siloxane D5 in this study was around one order of magnitude lower than the modeled values in urban areas in Chicago, Zurich, and Canada,<sup>69,70</sup> potentially due to emissions from sources other than leave-on PCPs in cities, such as industrial activities.<sup>69</sup>

VOC<sub>PTR</sub> concentrations in the return air were consistently higher than those in the supply air during the nighttime unoccupied periods throughout the campaign, indicating persistent emissions of VOCs from indoor surfaces and materials (Figure S9). The average increment in the VOC<sub>PTR</sub> concentration during the unoccupied periods was  $29.7 \mu\text{g m}^{-3}$ , equivalent to an emission rate of  $69.5 \mu\text{g h}^{-1}$  with the average outdoor volumetric airflow rate. The PMF analysis indicated that indoor surface-related emissions contributed ~38% to indoor VOC<sub>PTR</sub> concentrations during the entire campaign. Significant VOC emissions from new furniture and newly constructed or renovated rooms have been identified and characterized in numerous studies

(e.g., Brown<sup>71</sup>). However, since the building was constructed 5 years before the campaign and materials with minimal VOC emissions were chosen for the building in order to meet LEED criteria, significant off-gassing directly from furniture and finishing materials to office air is not expected.

The persistent emissions during unoccupied nighttime periods and the diverse range of emitted compounds indicated that their source is likely associated with an indoor surface reservoir. A previous study has demonstrated the universal existence of a substantial indoor surface reservoir for gas-phase contaminants via a series of enhanced ventilation experiments, where the repetitive rebounds of gas-phase contaminant concentrations were consistently observed after each enhanced ventilation period.<sup>72</sup> The authors indicated that most VOCs were accommodated in the condensed-phase surface reservoir, such as paints and organic films, rather than in indoor air, and can rapidly partition between two phases, thereby making the surface reservoir an emission source. A recent study showed continuous indoor emissions of VOCs in an unoccupied home, highlighting the existence of an abundant, long-lived indoor reservoir resulting from building materials and prior indoor use by occupants.<sup>10</sup> The office in this study contains various materials that permit reversible partitioning of VOCs between the room air and surface-phase, such as latex paint, fabrics, and other building materials,<sup>73–75</sup> thereby serving as a continuous emission source. In addition, except for the hard-tile flooring, which is cleaned periodically, other indoor surfaces, such as glass windows and desk surfaces, were not routinely cleaned. This may lead to the growth of a thick organic film layer and accumulation of deposited particles,<sup>76,77</sup> which can also serve as a substantial reservoir for VOCs. The persistent nighttime VOC emissions during the unoccupied periods indicate that the surface reservoir was never depleted during the measurement campaign.

A recent study demonstrated that liquid crystal display screens (e.g., used in laptops and monitors) can be an effective VOC source.<sup>78</sup> Used and new screens can emit a variety of alkanes, amides, alcohols, aldehydes, carboxylic acids, and liquid crystal monomers to indoor air with an emission rate of up to  $(8.25 \pm 0.90) \times 10^9 \text{ molecules s}^{-1} \text{ cm}^{-2}$ . Considering there were 28 monitors in the office, their contribution was not negligible. Small carboxylic acids, carbonyls, and alcohols (e.g., acetic acid, formic acid, formaldehyde, acetaldehyde, methanol, and acetone) contributed significantly to indoor surface-related emissions in the office, which agrees with previous indoor measurements with PTR-TOF-MS.<sup>21,28</sup> They may also be attributed

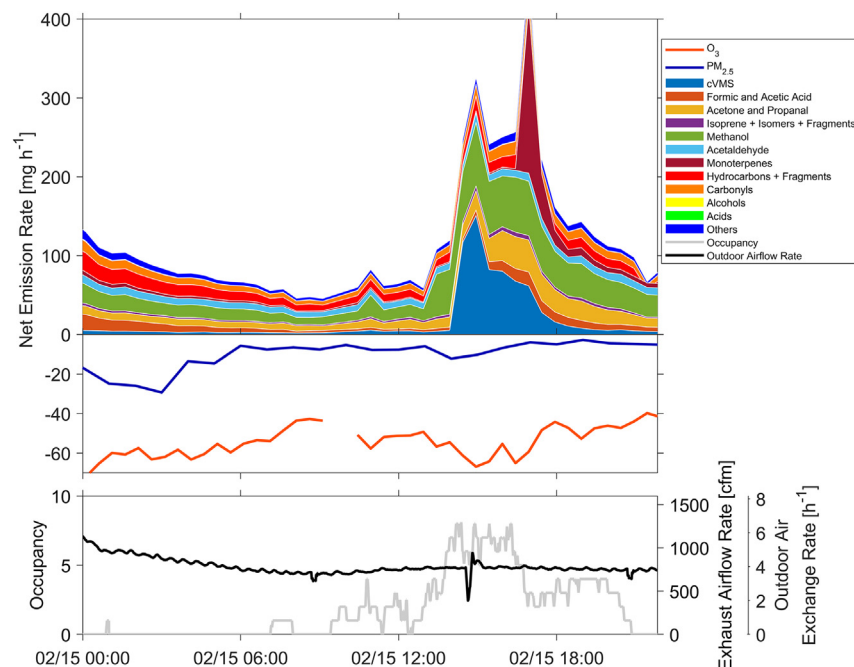


**Figure 4. Time-dependent changes in urban air pollutant exchange between indoor and outdoor atmospheric environments**

Temporal variations in the net emission rates of  $O_3$ ,  $PM_{2.5}$ , and VOCs (upper) and exhaust (outdoor) airflow rate and occupancy (lower) on February 15. Different colors represent different VOC types.

to wooden building materials and their degradation<sup>79</sup> and  $O_3$  reactions with indoor surfaces and furniture.<sup>65,80</sup>

### Temporal variations in net emission rates for VOCs, $O_3$ , and $PM_{2.5}$

The net emission rates for VOCs,  $O_3$ , and  $PM_{2.5}$  changed dynamically during the day. To demonstrate this, Figure 4 presents the time-series of  $E_{VOC_{PTR}}$ ,  $E_{PM_{2.5}}$ , and  $E_{Ozone}$  on one day during the measurement campaign, along with the exhaust (outdoor) air exchange rate and occupancy. The sine-like feature of the exhaust air exchange rate indicates that the ventilation system consistently adjusts the mixing ratio of recirculated and outdoor air in the supply air via the feedback control to maintain the mixed air temperature at the setpoint. The outdoor air exchange rate gradually decreased from 0:00 to 8:00, resulting in a decrease in the absolute value of net emission rates of the three air pollutants. The outdoor air exchange rate was relatively stable from 8:00 to midnight, during which  $E_{VOC_{PTR}}$  and  $E_{Ozone}$  were mainly influenced by occupancy. With the increase in occupancy from 0 to 8,  $E_{VOC_{PTR}}$  increased significantly from  $\sim 50$  to  $334 \text{ mg h}^{-1}$ . A sharp increase in the emission rate of cVMSs at  $\sim 14:00$  was especially evident, which could be associated with the entry of office workers who wore leave-on PCPs. The cVMS net emission rate gradually decreased during the day, as the PCP residue slowly wore off from the human envelope.<sup>26</sup> The emission rate of  $C_3H_6OH^+$  (acetone and propanal) and  $CH_4OH^+$  (methanol) remained elevated during the occupied period.

A sharp spike in the  $C_{10}H_{16}H^+$  (monoterpenes) net emission rate was observed at  $\sim 17:00$ , which dramatically increased  $E_{VOC_{PTR}}$ . We found a significant correlation (Pearson's  $r > 0.95$ ) of  $C_{10}H_{16}H^+$  with  $C_{10}H_{16}OH^+$  (potentially citral) and  $C_{10}H_{18}H^+$  (potentially methylisopropylcyclohexene), which are ions found in citrus peels, while a moderate correlation was observed with

$C_{10}H_{18}OH^+$  (potentially linalool or eucalyptol; Pearson's  $r = 0.64$ ), which is a fragrance compound commonly found in PCPs. Therefore, the spike in the monoterpene net emission rate may be associated with the consumption of citrus fruits rather than PCP use.<sup>21</sup> Episodic citrus fruit-associated monoterpene emissions were observed multiple times throughout the campaign. Conversely, on 2 days, we observed continuous emissions of monoterpenes with a magnitude much less than the citrus fruit-associated emissions, with a high correlation (Pearson's  $r > 0.85$ ) with  $C_{10}H_{16}OH^+$ ,  $C_{10}H_{18}H^+$ ,  $C_{10}H_{18}OH^+$ , and siloxane D5, potentially due to indoor

use of PCPs.  $E_{Ozone}$  declined from around  $-50$  to  $-66 \text{ mg h}^{-1}$  as occupancy changed from 0 to 8, due to an increase in occupant-associated surfaces, which contain reactive compounds produced by human sebaceous glands. However, the influence of occupancy on  $E_{Ozone}$  was not as dramatic as that on  $E_{VOC_{PTR}}$ .  $E_{PM_{2.5}}$  did not tend to vary with occupancy.

Figures S8 and S9 present an overview of the mean  $E_{Ozone}$ ,  $E_{VOC_{PTR}}$ , and  $E_{PM_{2.5}}$  during high-occupancy periods (10:00–18:00 on weekdays) and unoccupied periods at night. With a mean occupancy of 4.53 and a slightly higher mean outdoor airflow rate (by 13.6%),  $E_{Ozone}$  during the high-occupancy periods was 46.5% lower than that during unoccupied periods. The  $E_{PM_{2.5}}$  during unoccupied periods ( $-2.30 \text{ mg h}^{-1}$ ) was slightly lower than that during high-occupancy periods ( $-1.96 \text{ mg h}^{-1}$ ), potentially due to occupant-induced  $PM_{2.5}$  emissions (e.g., skin shedding and particle resuspension) and variations in outdoor  $PM_{2.5}$ . The total  $E_{VOC_{PTR}}$  during high-occupancy periods was  $121.3 \text{ mg h}^{-1}$ , which was 60% higher than the field campaign average ( $78.0 \text{ mg h}^{-1}$ ), with human- and PCP-related compounds (e.g., acetone, isoprene, cVMSs, 6-MHO) exhibiting significantly increased net emission rates. The relative contribution of each group of compounds to the total  $E_{VOC_{PTR}}$  also presents obvious temporal differences. Carbonyls and cVMSs contributed 30% and 13% to the total  $E_{VOC_{PTR}}$  during high-occupancy periods, respectively, compared with 29% and 3% during unoccupied periods. By contrast, the relative fraction of hydrocarbons, alcohols, and acids toward the total  $E_{VOC_{PTR}}$  was higher during the unoccupied periods.

### Relative importance of influencing factors on net emission rates

Due to changes in the operational conditions of the HVAC system, outdoor air pollutant concentrations, and occupancy, the



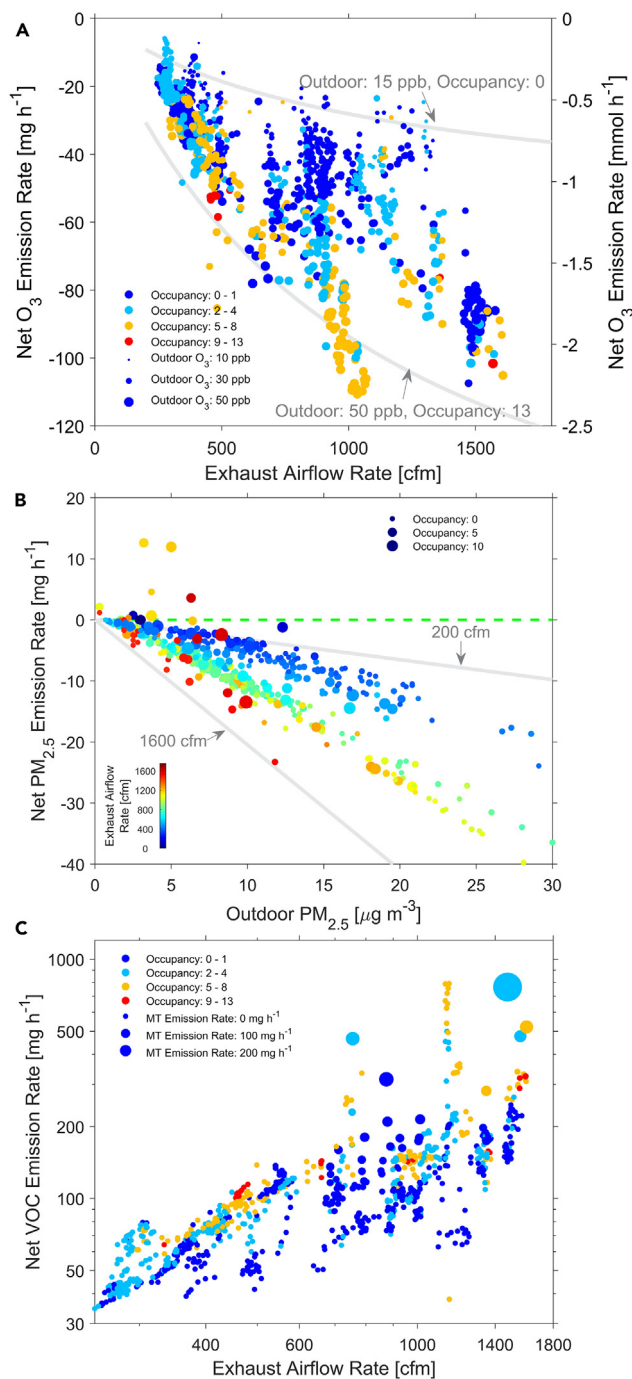


**Figure 5. Variations in urban air pollutant net emission rates with human occupancy, operational mode of the mechanical ventilation system, and outdoor air conditions**

(A) Scatterplot of  $E_{O_3}$  as a function of exhaust (outdoor) airflow rate. The color and size of the markers represent the occupancy and outdoor O<sub>3</sub> concentration, respectively. The two gray lines indicate the theoretical  $E_{O_3}$  under two assumed conditions including low outdoor O<sub>3</sub> concentration (15 ppb) with zero occupancy and high outdoor O<sub>3</sub> concentration (50 ppb) with high occupancy (13 occupants), which are calculated by using the O<sub>3</sub> indoor and human surface deposition velocities estimated in this study and assuming negligible gas-phase reactions.

values of  $E_{O_3}$ ,  $E_{VOC_{PTR}}$ , and  $E_{PM_{2.5}}$  varied over a wide range during the campaign (Table S3). In general,  $E_{O_3}$  and  $E_{PM_{2.5}}$  decrease as the exhaust (outdoor) airflow rate increases, while  $E_{VOC_{PTR}}$  increases with exhaust airflow rate (Figure 5). These trends indicate how mechanically ventilated buildings can remove increasing amounts of urban O<sub>3</sub> and PM<sub>2.5</sub> as the outdoor air exchange rate increases; however, this leads to greater transport of indoor-generated VOCs to the urban atmosphere.

Figure 5A presents  $E_{O_3}$  as a function of the exhaust airflow rate, with markers color-coded by occupancy. The marker size indicates outdoor O<sub>3</sub> concentrations. The two reference lines suggest the theoretical  $E_{O_3}$  calculated using the estimated O<sub>3</sub> surface and human deposition velocity in this study at the steady state and given outdoor O<sub>3</sub> concentration and occupancy, assuming negligible O<sub>3</sub> reactions in the gas phase (details in the supplemental information). The observed  $E_{O_3}$  generally lies within the two assumed conditions, including high outdoor O<sub>3</sub> concentrations with high occupancy (outdoor O<sub>3</sub> of 50 ppb and 13 occupants) and low outdoor O<sub>3</sub> concentrations with no occupancy (outdoor O<sub>3</sub> of 15 ppb and 0 occupants). At a given exhaust airflow rate,  $E_{O_3}$  tended to decrease with the increase in occupancy and outdoor O<sub>3</sub> concentrations. Relative importance (RI) analysis<sup>81</sup> was conducted (details in the supplemental information) to identify the most influencing factor that led to the significant variations in  $E_{O_3}$  (5<sup>th</sup> to 95<sup>th</sup>: -88.8 to -17.6 mg h<sup>-1</sup>). The results indicated that the exhaust airflow rate accounted for 70.3% of the variance observed in  $E_{O_3}$ , followed by the outdoor O<sub>3</sub> concentration (24.6%), and occupancy (4.91%), while the indoor monoterpene concentration had a negligible influence (<1%).

Figure 5B shows  $E_{PM_{2.5}}$  as a function of the outdoor PM<sub>2.5</sub> concentration, with markers color-coded by the exhaust airflow rate. The two reference lines indicate the estimated theoretical  $E_{PM_{2.5}}$  at steady state at the highest and lowest outdoor airflow rates, assuming that filtration is the only removal mechanism and there are no indoor emissions of PM<sub>2.5</sub> in the office (details in the supplemental information). To calculate the theoretical  $E_{PM_{2.5}}$ , the filtration efficiencies of the MERV 8 and MERV 14 filters from Azimi et al. were adopted.<sup>12</sup> The values of  $E_{PM_{2.5}}$  were occasionally positive during the campaign. The measured indoor particle size distributions indicated that they were due to occasional intense indoor emissions of particles larger than 1 μm, likely associated with occupant activities.  $E_{PM_{2.5}}$  decreased with the increase of outdoor PM<sub>2.5</sub> concentration and outdoor airflow rate, indicating that the building and the HVAC system remove more PM<sub>2.5</sub> from the urban atmosphere with a higher incoming mass flux of PM<sub>2.5</sub> into the outdoor air intake. RI analysis indicates that the outdoor PM<sub>2.5</sub> concentration contributed to 88.4% of

(B) Scatterplot of  $E_{PM_{2.5}}$  as a function of the outdoor PM<sub>2.5</sub> concentration. The color and size of the markers represent the exhaust (outdoor) airflow rate and occupancy, respectively. The two gray lines indicate the theoretical  $E_{PM_{2.5}}$ , assuming HVAC filtration is the only loss mechanism of incoming outdoor PM<sub>2.5</sub>. The filtration efficiency of the two HVAC filters was adopted from Azimi et al.<sup>12</sup>

(C) Scatterplot of  $E_{VOC_{PTR}}$  as a function of exhaust (outdoor) airflow rate on a log-log scale. The color and size of the markers represent the occupancy and monoterpene emission rates, respectively.

the variance of  $E_{PM_{2.5}}$ , followed by the outdoor airflow rate (11.1%), while the influence of occupancy was negligible (<1%).

Figure 5C shows that  $E_{VOC_{PTR}}$  spanned more than an order of magnitude, from  $\sim 30$  to  $700 \text{ mg h}^{-1}$ .  $E_{VOC_{PTR}}$  generally increases with occupancy (color-coded markers), while episodic monoterpene emissions due to occupant activities dramatically enhanced the transient  $E_{VOC_{PTR}}$  (noted by the size of the markers).  $E_{VOC_{PTR}}$  also increases with the exhaust airflow rate, since greater dilution of indoor air by outdoor airflow drives the VOCs to partition from indoor surface reservoirs to the gas phase and lead to greater indoor surface emissions.<sup>72</sup> Higher exhaust airflow rates also lead to higher indoor  $O_3$  concentrations, since the main source of indoor  $O_3$  is outdoor transport. This facilitates the reactions of  $O_3$  with indoor and human surfaces to produce a variety of VOCs (e.g., hexanal, 6-MHO, and geranyl acetone), later being flushed to the urban atmosphere. The RI analysis indicates that the exhaust airflow rate contributed to 67% of the variance of  $E_{VOC_{PTR}}$ , followed by occupant-induced episodic monoterpene emissions (17%) and occupancy (15%).

#### Study limitations, implications, and future outlook

In this study, we reported the  $E_{VOC_{PTR}}$  for the product ions, to which we assigned chemical formulas based on the measured  $m/z$ , from the proton transfer reactions between VOCs and  $H_3O^+$  in the PTR-TOF-MS. However, caution is needed when interpreting the data as the reported product ions may not be the protonated parent compounds but fragment ions due to fragmentation reactions. Although we have corrected for the fragments when estimating the mixing ratios for the compounds with calibration standards, such as 6-MHO, monoterpenes, and siloxane D5 (details in the supplemental information; Table S4), we were not able to do that for the uncalibrated compounds. This may lead to an underestimation in the  $VOC_{PTR}$  mixing ratios and the magnitude of  $E_{VOC_{PTR}}$  for compounds for which fragmentation reactions take place, such as long-chain aldehydes (e.g., hexanal), which have been shown to be important indoor VOCs.<sup>22,31,32</sup> We have attributed some ions in Figure 1 and Table S1 to potential fragments of long-chain aldehydes (e.g.,  $C_7H_{12}H^+$  as a heptanal fragment). Fragmentation will also bias the fractions of carbonyls, alcohols, and acids in Figures 1 and 4, as some of them may be classified under the “hydrocarbons and fragments” category. On the other hand, a neutral water molecule is lost in most of the fragmentation reactions, which resulted in an underestimation in the total  $E_{VOC_{PTR}}$ . However, we do not expect this underestimation to be significant as the molecular weight of water is relatively small compared with the long-chain aldehydes.

When estimating the  $VOC_{PTR}$  mixing ratios from the PTR-TOF-MS measurements, we calibrated for important VOCs known to be emitted or formed indoors, including methanol, acetone, siloxane D5, monoterpenes, isoprene, toluene, and decanal, with a collection of 21 authentic calibration standards (Table S4). This approach is consistent with the majority of field studies employing online mass spectrometry for real-time measurement of VOCs in indoor atmospheric environments. Uncalibrated species were assumed to have sensitivities equivalent to a single proton transfer rate constant. Although certain compounds (e.g., ethanol and trichlorobenzene) exhibit much lower sensitivities than assumed, the VOC concentration estimated

in this manner is generally considered to have an uncertainty of around  $\pm 50\%$  for individual compounds.<sup>21,28</sup> Thus, net emission rates for ethanol are likely underestimates of their true values. However, the overall uncertainties on the total  $E_{VOC_{PTR}}$  may largely cancel. Given the complexity of the entire building system, including VOC emissions and transformations, occupancy and occupant activities, and ventilation flows and conditions, all of which were carefully monitored in real-time, the underestimated ethanol concentrations do not strongly influence the conclusions of this study and the reported total  $E_{VOC_{PTR}}$ . On the other hand, the reported  $E_{VOC_{PTR}}$  only accounts for VOCs that can be monitored by the deployed PTR-TOF-MS operating in  $H_3O^+$  mode. It is known that VOCs with proton affinities lower than water cannot be effectively detected by the PTR-TOF-MS, such as alkanes.<sup>82</sup> Therefore, the reported  $E_{VOC_{PTR}}$  does not include all VOCs present in the office and represents a lower bound of the actual net emission rate for VOCs from the office to the urban atmosphere. In the future, PTR-TOF-MS measurements under different reagent ion modes ( $O_2^+$ ,  $NO^+$ , and  $NH_4^+$ ) and calibration of the PTR-TOF-MS with a greater number of authentic standards can provide a more complete assessment of the VOC mass flux between buildings and outdoor air.

We demonstrated the source and sink effect of modern buildings on urban air pollutants by reporting the net emission rates of the selected urban air pollutants in an open-plan office in a LEED-certified high-performance building through a 1-month measurement campaign. However, the net emission rates of air pollutants from buildings to the urban atmosphere will vary for different types of buildings (e.g., residential buildings, restaurants, and hospitals), different configurations (e.g., single-pass mechanical ventilation and grade of filters) and operational conditions (e.g., control logic) of the HVAC systems, and occupant behaviors. Buildings with strong indoor emission sources would exhibit dramatically different net emission patterns. For example, commercial kitchens are expected to emit significant quantities of particulate matter, VOCs, and reactive nitrogen compounds into the urban atmosphere, resulting in a much higher  $E_{VOC}$  and potentially a positive value of  $E_{PM_{2.5}}$ .<sup>83,84</sup>

The design and operational conditions of the ventilation system are key factors affecting the source and sink behaviors of buildings as they govern the air exchange between buildings and the urban atmosphere. For example, the ventilation system of the office operates differently in the cooling season compared with the heating season, during which the study was conducted, further influencing the regulation of exhaust/intake airflow. During the cooling season, the system still keeps the supply air exchange rate at  $\sim 7 \text{ h}^{-1}$ . When indoor air temperature > mixed air temperature setpoint > outdoor air temperature, the system adopts the mixed air temperature control, similar to the heating season. However, since the outdoor air temperature is generally higher during the cooling season than the heating season, we expect higher exhaust airflow rates to maintain the mixed air temperature at the setpoint, which facilitates the exchange of air pollutants between the office and the urban atmosphere. When indoor air temperature > outdoor air temperature > mixed air temperature setpoint, the system adopts 100% outdoor air and the exhaust/intake airflow rates are equal to the supply airflow rate, where the exchange of air pollutants reaches the maximum. When the

outdoor air temperature further increases and outdoor air temperature > indoor air temperature setpoint, the system will automatically decrease the exhaust airflow rate to around half of the supply airflow rate in order to recirculate a part of the room air to maintain the indoor air temperature at the setpoint, which suppresses air exchange. Although the HVAC system of the office allows room air recirculation, buildings with single-pass mechanical ventilation systems may interact with the urban atmosphere differently. Tang et al.<sup>21</sup> performed an indoor air chemistry study in a university classroom where a single-pass mechanical ventilation system provided outdoor airflow at a fixed room air exchange rate of  $5 \text{ h}^{-1}$ . In such a case, the net emission rate would depend on factors such as the outdoor concentration of air pollutants, filters used in the HVAC system, and indoor occupancy and activities rather than exhaust airflow rate.<sup>21</sup>

Aside from the difference in operational conditions of the HVAC system between cooling and heating seasons, there are other seasonal variations in factors that can affect the net emission rates. For example, we observed an  $\text{O}_3$  deposition velocity of  $1.35 \pm 0.63 \text{ cm s}^{-1}$  to the human body in this study, which is 2–6 times higher than the values in the literature.<sup>35,36,85–87</sup> It is likely attributed to the multiple layers of soiled winter clothing worn by the office workers during the wintertime. We would expect a lower deposition velocity during the summertime due to less clothing. However, this may not necessarily lead to a lower  $E_{\text{ozone}}$  since the outdoor  $\text{O}_3$  concentration is expected to be higher during the summertime, resulting in a greater  $\text{O}_3$  intake mass flux. In addition, moisture can condense on cooling coils in the HVAC system during the summertime to form a water film layer and condensate in the duct. They may act as a sink for water-soluble organic gases (WSOGs),<sup>88</sup> which would reduce the net emission rates of WSOG from buildings to the urban atmosphere.

Through direct measurements, we observed dynamic source and sink effects of the office for urban air pollutants. However, it is still difficult to assess the overall impact of the air exchange between buildings and the urban atmosphere on urban air pollution based on this study. For example, due to the reactions of  $\text{O}_3$  with indoor and human surfaces, the office acts as a sink for urban  $\text{O}_3$ . However, these reactions produce a variety of VOCs<sup>34,36</sup> and potentially particulate matter,<sup>89</sup> which are released to the urban atmosphere. We found VOC molar yields of 0.048, 0.018, and 0.024 for 6-MHO, 4-OPA, and decanal, respectively, upon  $\text{O}_3$  uptake onto human body surfaces based on our earlier analysis of the same data from our PTR-TOF-MS measurements.<sup>39</sup> On the other hand, although the office acts as a sink for  $\text{PM}_{2.5}$  and  $\text{O}_3$  and a source for VOCs for the urban atmosphere, the released VOCs can contribute to the reactivity of outdoor air and undergo photochemical reactions to contribute to  $\text{O}_3$  and SOA formation in urban environments, especially for reactive VOCs from PCPs and VCPs, such as monoterpenes, monoterpenoids, and sesquiterpenes, which can offset the  $E_{\text{PM}_{2.5}}$  and  $E_{\text{ozone}}$  to an unknown extent. To comprehensively understand the overall impact of building ventilation on urban air pollution on a city scale, collaborative research can be conducted to (1) measure the net emission rates of air pollutants from different types of buildings with different ventilation conditions; (2) experimentally study the

fate and transformation of building-originated air pollutants in the urban atmosphere; (3) perform a wide survey of building use patterns, building occupancy, and configuration and operational conditions of HVAC systems in a city; and (4) develop an atmospheric chemistry model based on the results from the above-mentioned studies to estimate the overall effect of building ventilation on urban air pollution.

The results of this study have potential implications for strategies for better controlling and mitigating the negative impact of buildings on urban air quality. Equipping the HVAC system with activated carbon filters and higher-grade particulate filters would provide improved indoor air quality. At the same time, it facilitates the removal of  $\text{O}_3$  and particulate matter from the urban atmosphere. Reducing indoor  $\text{O}_3$  concentrations also suppress the secondary formation of VOCs<sup>34,36</sup> and particulate matter from the reactions with gas-phase reactive VOCs (e.g., monoterpenes from VCPs) and indoor and human surfaces, further decreasing the magnitude of VOC and aerosol fluxes from buildings to the urban atmosphere. Implementing in-room air cleaning technologies, such as photocatalytic purification and portable filtration devices, would reduce particulate matter and VOCs released to the urban atmosphere. However, the above-mentioned strategies would increase energy consumption and cost for building operators and owners. On the other hand, given the significant use of PCPs and VCPs in indoor environments, VOC emission standards for such products can be established to reduce their emissions from buildings to the urban atmosphere, especially for VOCs with enhanced reactivities, such as monoterpenes, sesquiterpenes, and their derivatives.

This study provides a framework that can be reproduced to estimate the net emission rates of target air pollutants from buildings to the urban atmosphere. To enable network measurements at multiple sites, sensor arrays with low-cost  $\text{PM}_{2.5}$ , VOC, and  $\text{O}_3$  sensors can be used in HVAC systems to estimate net emission rates. Such data can be coupled with building automation system data on intake/exhaust airflow rates and occupancy to provide insights into the impact of building systems and occupants on net emission rates for a diverse collection of buildings. Furthermore, month-long measurement campaigns similar to this study can deploy high-resolution online mass spectrometry, including PTR-TOF-MS and aerosol mass spectrometry, to determine speciated net emission rates for reactive gases and particulate matter, respectively.

## EXPERIMENTAL PROCEDURES

### Resource availability

#### Lead contact

Further information and requests for resources and reagents should be directed to and will be fulfilled by the lead contact, Brandon E. Boor ([bboor@purdue.edu](mailto:bboor@purdue.edu)).

#### Materials availability

This study did not generate new, unique materials.

#### Data and code availability

All data needed to evaluate the conclusions in the paper are present in the main paper and/or the [supplemental information](#). All data for the figures in the main paper and/or the [supplemental information](#) are available from the [lead contact](#) upon reasonable request. Custom code for this work is available from the [lead contact](#) upon reasonable request.

## Site description: Herrick Living Laboratory Office at Purdue University

The study site is a realistic, modern open-plan office located in a LEED Gold-certified building, which was designed and built to meet criteria for future green and high-performance buildings.<sup>90–92</sup> The office has a maximum occupancy of 20, and there is no fixed working schedule for the office workers. The floor area is 104 m<sup>2</sup>. The interior is furnished with materials with significantly reduced or negligible VOC emissions. To keep the results representative and realistic, deliberate disturbances and interventions that could affect indoor air chemistry and building operation were minimized.

## Air pollutant measurements and instrumentation

VOCs with a proton affinity greater than water were monitored by a PTR-TOF-MS (PTR-TOF 4000, Ionicon Analytik, Innsbruck, Austria) using H<sub>3</sub>O<sup>+</sup> as the reagent ion.<sup>15–19,24,39,93</sup> O<sub>3</sub> concentrations were monitored by an O<sub>3</sub> gas analyzer (M400E, Teledyne Technologies, Thousand Oaks, CA, US) with a precision of 1 ppb. To estimate the net emission rates, VOC and O<sub>3</sub> concentrations were monitored in both the outdoor air and return air ducts via a continuously purged multi-port valve system (details in the [supplemental information](#)). Perfluoroalkoxy (PFA) tubes (3/8" outside diameter [OD]) were used as the sampling lines, connecting the sampling location to the multi-port valve. A polytetrafluoroethylene (PTFE) membrane filter was installed at the inlet of each sampling line to remove particles. The residence time of the sample air was no more than 4 s in the sampling lines. The PTR-TOF-MS was calibrated daily using 21 calibration gas standards, including common indoor VOCs such as methanol, acetone, siloxane D5, monoterpenes, isoprene, toluene, and decanal ([Table S4](#)). We were not able to calibrate the PTR-TOF-MS for other common indoor VOCs, such as ethanol. Thus, uncertainties in the reported mixing ratios and net mass emission rates for ethanol are expected to be greater than for the calibrated species, as discussed in the “[study limitations, implications, and future outlook](#)” section.

Indoor particle number size distributions from 10 to 300 nm were measured by a scanning mobility particle sizer (SMPS; Model 3910, TSI, Shoreview, MN, US).<sup>94</sup> Particle number size distributions from 300 to 10,000 nm were measured by an optical particle sizer (OPS; Model 3330, TSI, Shoreview, MN, US).<sup>95</sup> The SMPS and OPS were placed on the north side of the office with the inlet at a height of ~1.3 m. The measured indoor particle number size distributions were converted to mass size distributions and integrated to calculate indoor PM<sub>2.5</sub> mass concentrations (details in the [supplemental information](#)).

## Estimation of net emission rates for VOCs, O<sub>3</sub>, and PM<sub>2.5</sub>

The net mass emission rates for VOCs, O<sub>3</sub>, and PM<sub>2.5</sub> from the office and its HVAC system to the proximate urban atmosphere were calculated using the following equation:

$$E_{net,j} = [Air\ Pollutant]_{i,exhaust} \times Q_{exhaust} - [Air\ Pollutant]_{i,intake} \times Q_{intake} \quad (\text{Equation 1})$$

where  $E_{net,j}$  represents the net mass emission rate (mg h<sup>-1</sup>) of air pollutant  $j$ ;  $[Air\ Pollutant]_j$  is the mass concentration of air pollutant  $i$  (mg m<sup>-3</sup>) in the exhaust or intake airflow of the HVAC system; and  $Q_{exhaust}$  and  $Q_{intake}$  represent the exhaust and intake volumetric airflow rates (m<sup>3</sup> h<sup>-1</sup>) in the HVAC system, respectively.  $E_{VOC_{PTR}}$ ,  $E_{ozone}$ , and  $E_{PM_{2.5}}$  are used to refer to the net emission rates for each air pollutant category.

For VOCs and O<sub>3</sub>, the concentration measured in the outdoor air duct was used as the intake airflow concentration. The return air concentration was used as the exhaust airflow concentration. The PM<sub>2.5</sub> mass concentration measured by the local US EPA monitoring station was obtained and used as the concentration in the intake airflow. The indoor PM<sub>2.5</sub> mass concentration derived from the SMPS and OPS measurements in the office was used as the concentration being exhausted from the building. The volumetric airflow rates of the exhaust and intake air were measured by air velocity mass flow transducers with a time resolution of 1 min and an accuracy of ±2%. Additional details are provided in the [supplemental information](#).

## SUPPLEMENTAL INFORMATION

Supplemental information can be found online at <https://doi.org/10.1016/j.crsus.2024.100103>.

## ACKNOWLEDGMENTS

Financial support was provided by the National Science Foundation (CBET-1847493 and CBET-1805804 to B.E.B.) and the Alfred P. Sloan Foundation Chemistry of the Indoor Environments Program (G-2018-11061 to B.E.B. and P.S.S.). The authors would like to thank the staff at the Ray W. Herrick Laboratories for their support in conducting the air pollutant measurements in the Herrick Living Laboratory office.

## AUTHOR CONTRIBUTIONS

B.E.B., T.W., and P.S.S. designed the study. T.W., A.T., D.N.W., J.J., H.J.H., P.S.S., N.J., and B.E.B. conducted the study and collected the data. T.W. and A.T. analyzed the data. T.W. and B.E.B. wrote the manuscript with input from all coauthors. B.E.B. managed the research project.

## DECLARATION OF INTERESTS

The authors declare no competing interests.

Received: January 29, 2024

Revised: April 5, 2024

Accepted: April 29, 2024

Published: May 24, 2024

## REFERENCES

- Daellenbach, K.R., Kourtchev, I., Vogel, A.L., Bruns, E.A., Jiang, J., Petäjä, T., Jaffrezo, J.-L., Aksoyoglu, S., Kalberer, M., Baltensperger, U., et al. (2019). Impact of anthropogenic and biogenic sources on the seasonal variation in the molecular composition of urban organic aerosols: a field and laboratory study using ultra-high-resolution mass spectrometry. *Atmos. Chem. Phys.* *19*, 5973–5991.
- Li, N., He, Q., Greenberg, J., Guenther, A., Li, J., Cao, J., Wang, J., Liao, H., Wang, Q., and Zhang, Q. (2018). Impacts of biogenic and anthropogenic emissions on summertime ozone formation in the Guanzhong Basin, China. *Atmos. Chem. Phys.* *18*, 7489–7507.
- Gu, S., Guenther, A., and Faiola, C. (2021). Effects of anthropogenic and biogenic volatile organic compounds on Los Angeles air quality. *Environ. Sci. Technol.* *55*, 12191–12201.
- Yuan, B., Shao, M., De Gouw, J., Parrish, D.D., Lu, S., Wang, M., Zeng, L., Zhang, Q., Song, Y., Zhang, J., et al. (2012). Volatile organic compounds (VOCs) in urban air: How chemistry affects the interpretation of positive matrix factorization (PMF) analysis. *J. Geophys. Res.* *117*, D24302.
- Fenger, J. (1999). Urban air quality. *Atmos. Environ.* *33*, 4877–4900.
- Gkatzelis, G.I., Coggon, M.M., McDonald, B.C., Peischl, J., Aikin, K.C., Gilman, J.B., Trainer, M., and Warneke, C. (2021). Identifying Volatile Chemical Product Tracer Compounds in U.S. Cities. *Environ. Sci. Technol.* *55*, 188–199.
- Coggon, M.M., McDonald, B.C., Vlasenko, A., Veres, P.R., Bernard, F., Koss, A.R., Yuan, B., Gilman, J.B., Peischl, J., Aikin, K.C., et al. (2018). Diurnal variability and emission pattern of decamethylcyclopentasiloxane (D5) from the application of personal care products in two North American cities. *Environ. Sci. Technol.* *52*, 5610–5618.
- Gkatzelis, G.I., Coggon, M.M., McDonald, B.C., Peischl, J., Gilman, J.B., Aikin, K.C., Robinson, M.A., Canonaco, F., Prevot, A.S.H., Trainer, M., et al. (2021). Observations confirm that volatile chemical products are a major source of petrochemical emissions in U.S. cities. *Environ. Sci. Technol.* *55*, 4332–4343.

9. Coggon, M.M., Gkatzelis, G.I., McDonald, B.C., Gilman, J.B., Schwantes, R.H., Abuhassan, N., Aikin, K.C., Arend, M.F., Berkoff, T.A., Brown, S.S., et al. (2021). Volatile chemical product emissions enhance ozone and modulate urban chemistry. *Proc. Natl. Acad. Sci. USA* *118*, e2026653118.
10. Sheu, R., Fortenberry, C.F., Walker, M.J., Eftekhari, A., Stönnner, C., Bakker, A., Peccia, J., Williams, J., Morrison, G.C., Williams, B.J., et al. (2021). Evaluating indoor air chemical diversity, indoor-to-outdoor emissions, and surface reservoirs using high-resolution mass spectrometry. *Environ. Sci. Technol.* *55*, 10255–10267.
11. Stinson, B., Laguerre, A., and Gall, E.T. (2022). Per-person and whole-building VOC emission factors in an occupied school with gas-phase air cleaning. *Environ. Sci. Technol.* *56*, 3354–3364.
12. Azimi, P., Zhao, D., and Stephens, B. (2014). Estimates of HVAC filtration efficiency for fine and ultrafine particles of outdoor origin. *Atmos. Environ.* *98*, 337–346.
13. Avery, A.M., Waring, M.S., and DeCarlo, P.F. (2019). Seasonal variation in aerosol composition and concentration upon transport from the outdoor to indoor environment. *Environ. Sci. Process Impacts* *21*, 528–547.
14. Shen, J., and Gao, Z. (2018). Ozone removal on building material surface: A literature review. *Build. Environ.* *134*, 205–217.
15. Jiang, J., Ding, X., Tasoglou, A., Huber, H., Shah, A.D., Jung, N., and Boor, B.E. (2021). Real-time measurements of botanical disinfectant emissions, transformations, and multiphase inhalation exposures in buildings. *Environ. Sci. Technol. Lett.* *8*, 558–566.
16. Jiang, J., Ding, X., Isaacson, K.P., Tasoglou, A., Huber, H., Shah, A.D., Jung, N., and Boor, B.E. (2021). Ethanol-based disinfectant sprays drive rapid changes in the chemical composition of indoor air in residential buildings. *J. Hazard. Mater. Lett.* *2*, 100042.
17. Ding, X., Lu, H., Jiang, J., Tasoglou, A., Shah, A.D., and Jung, N. (2023). Real-time indoor sensing of volatile organic compounds during building disinfection events via photoionization detection and proton transfer reaction mass spectrometry. *Build. Environ.* *246*, 110953.
18. Rosales, C.M.F., Jiang, J., Lahib, A., Bottorff, B.P., Reidy, E.K., Kumar, V., Tasoglou, A., Huber, H., Dusanter, S., Tomas, A., et al. (2022). Chemistry and human exposure implications of secondary organic aerosol production from indoor terpene ozonolysis. *Sci. Adv.* *8*, eabj9156.
19. Liu, J., Jiang, J., Ding, X., Patra, S.S., Cross, J.N., Huang, C., Kumar, V., Price, P., Reidy, E.K., Tasoglou, A., et al. (2024). Real-time evaluation of terpene emissions and exposures during the use of scented wax products in residential buildings with PTR-TOF-MS. *Build. Environ.* *255*, 111314.
20. Yeoman, A.M., Shaw, M., and Lewis, A.C. (2021). Estimating person-to-person variability in VOC emissions from personal care products used during showering. *Indoor Air* *31*, 1281–1291.
21. Tang, X., Misztal, P.K., Nazaroff, W.W., and Goldstein, A.H. (2016). Volatile organic compound emissions from humans indoors. *Environ. Sci. Technol.* *50*, 12686–12694.
22. Arata, C., Misztal, P.K., Tian, Y., Lunderberg, D.M., Kristensen, K., Novoselac, A., Vance, M.E., Farmer, D.K., Nazaroff, W.W., and Goldstein, A.H. (2021). Volatile organic compound emissions during HOMEChem. *Indoor Air* *31*, 2099–2117.
23. Logue, J.M., McKone, T.E., Sherman, M.H., and Singer, B.C. (2011). Hazard assessment of chemical air contaminants measured in residences. *Indoor Air* *21*, 92–109.
24. Jiang, J., Ding, X., Patra, S.S., Cross, J.N., Huang, C., Kumar, V., Price, P., Reidy, E.K., Tasoglou, A., Huber, H., et al. (2023). Siloxane emissions and exposures during the use of hair care products in buildings. *Environ. Sci. Technol.* *57*, 19999–20009.
25. McDonald, B.C., De Gouw, J.A., Gilman, J.B., Jathar, S.H., Akherati, A., Cappa, C.D., Jimenez, J.L., Lee-Taylor, J., Hayes, P.L., McKeen, S.A., et al. (2018). Volatile chemical products emerging as largest petrochemical source of urban organic emissions. *Science* *359*, 760–764.
26. Tang, X., Misztal, P.K., Nazaroff, W.W., and Goldstein, A.H. (2015). Siloxanes are the most abundant volatile organic compound emitted from engineering students in a classroom. *Environ. Sci. Technol. Lett.* *2*, 303–307.
27. Finewax, Z., Pagonis, D., Clafin, M.S., Handschy, A.V., Brown, W.L., Jenks, O., Nault, B.A., Day, D.A., Lerner, B.M., and Jimenez, J.L. (2021). Quantification and source characterization of volatile organic compounds from exercising and application of chlorine-based cleaning products in a university athletic center. *Indoor Air* *31*, 1323–1339.
28. Liu, Y., Misztal, P.K., Xiong, J., Tian, Y., Arata, C., Weber, R.J., Nazaroff, W.W., and Goldstein, A.H. (2019). Characterizing sources and emissions of volatile organic compounds in a northern California residence using space- and time-resolved measurements. *Indoor Air* *29*, 630–644.
29. Molinier, B., Arata, C., Katz, E.F., Lunderberg, D.M., Liu, Y., Misztal, P.K., Nazaroff, W.W., and Goldstein, A.H. (2022). Volatile methyl siloxanes and other organosilicon compounds in residential air. *Environ. Sci. Technol.* *56*, 15427–15436.
30. Weschler, C.J., and Carslaw, N. (2018). Indoor chemistry. *Environ. Sci. Technol.* *52*, 2419–2428.
31. Kruza, M., Lewis, A.C., Morrison, G.C., and Carslaw, N. (2017). Impact of surface ozone interactions on indoor air chemistry: A modeling study. *Indoor Air* *27*, 1001–1011.
32. Liu, Y., Misztal, P.K., Arata, C., Weschler, C.J., Nazaroff, W.W., and Goldstein, A.H. (2021). Observing ozone chemistry in an occupied residence. *Proc. Natl. Acad. Sci. USA* *118*, e2018140118.
33. Wang, N., Zannoni, N., Ernle, L., Bekö, G., Wargocki, P., Li, M., Weschler, C.J., and Williams, J. (2021). Total OH reactivity of emissions from humans: In situ measurement and budget analysis. *Environ. Sci. Technol.* *55*, 149–159.
34. Wang, N., Ernle, L., Bekö, G., Wargocki, P., and Williams, J. (2022). Emission rates of volatile organic compounds from humans. *Environ. Sci. Technol.* *56*, 4838–4848.
35. Pagonis, D., Price, D.J., Algrim, L.B., Day, D.A., Handschy, A.V., Stark, H., Miller, S.L., de Gouw, J.A., Jimenez, J.L., and Ziemann, P.J. (2019). Time-resolved measurements of indoor chemical emissions, deposition, and reactions in a university art museum. *Environ. Sci. Technol.* *53*, 4794–4802.
36. Wisthaler, A., and Weschler, C.J. (2010). Reactions of ozone with human skin lipids: sources of carbonyls, dicarbonyls, and hydroxycarbonyls in indoor air. *Proc. Natl. Acad. Sci. USA* *107*, 6568–6575.
37. Weschler, C.J. (2016). Roles of the human occupant in indoor chemistry. *Indoor Air* *26*, 6–24.
38. Du Bois, D., and Du Bois, E.F. (1989). A formula to estimate the approximate surface area if height and weight be known. 1916. *Nutrition* *5*, 303–311. discussion 312–313.
39. Wu, T., Tasoglou, A., Huber, H., Stevens, P.S., and Boor, B.E. (2021). Influence of mechanical ventilation systems and human occupancy on time-resolved source rates of volatile skin oil ozonolysis products in a LEED-certified office building. *Environ. Sci. Technol.* *55*, 16477–16488.
40. Weschler, C.J. (2000). Ozone in indoor environments: concentration and chemistry. *Indoor Air* *10*, 269–288.
41. Deming, B.L., and Ziemann, P.J. (2020). Quantification of alkenes on indoor surfaces and implications for chemical sources and sinks. *Indoor Air* *30*, 914–924.
42. Nicolaidis, N. (1974). Skin lipids: their biochemical uniqueness. *Science* *186*, 19–26.
43. Weber, S.U., Thiele, J.J., Cross, C.E., and Packer, L. (1999). Vitamin C, uric acid, and glutathione gradients in murine stratum corneum and their susceptibility to ozone exposure. *J. Invest. Dermatol.* *113*, 1128–1132.
44. Guo, C., Gao, Z., and Shen, J. (2019). Emission rates of indoor ozone emission devices: A literature review. *Build. Environ.* *158*, 302–318.
45. Hecker, R., and Hofacre, K.C. (2008). Development of Performance Data for Common Building Air Cleaning Devices. Final Report No. EPA/600/R-08/013 (US Environmental Protection Agency, Office of Research and Development/National Homeland Security Research Center Research).

46. Lai, A.C.K., and Nazaroff, W.W. (2000). Modeling indoor particle deposition from turbulent flow onto smooth surfaces. *J. Aerosol Sci.* *31*, 463–476.
47. Nazaroff, W.W. (2004). Indoor particle dynamics. *Indoor Air* *14*, 175–183. Suppl 7.
48. Patra, S.S., Jiang, J., Ding, X., Huang, C., Reidy, E.K., Kumar, V., Price, P., Keech, C., Steiner, G., Stevens, P.S., et al. (2024). Dynamics of nanocluster aerosol in the indoor atmosphere during gas cooking. *PNAS Nexus* *3*, pgae044.
49. Wagner, D.N., Odhiambo, S.R., Ayikukwei, R.M., and Boor, B.E. (2022). High time-resolution measurements of ultrafine and fine woodsmoke aerosol number and surface area concentrations in biomass burning kitchens: a case study in western Kenya. *Indoor Air* *32*, e13132.
50. Patra, S.S., Wu, T., Wagner, D.N., Jiang, J., and Boor, B.E. (2021). Real-time measurements of fluorescent aerosol particles in a living laboratory office under variable human occupancy and ventilation conditions. *Build. Environ.* *205*, 108249.
51. Wu, T., Fu, M., Valkonen, M., Täubel, M., Xu, Y., and Boor, B.E. (2021). Particle resuspension dynamics in the infant near-floor microenvironment. *Environ. Sci. Technol.* *55*, 1864–1875.
52. Bhangar, S., Adams, R.I., Pasut, W., Huffman, J.A., Arens, E.A., Taylor, J.W., Bruns, T.D., and Nazaroff, W.W. (2016). Chamber bioaerosol study: Human emissions of size-resolved fluorescent biological aerosol particles. *Indoor Air* *26*, 193–206.
53. Morawska, L., Xiu, M., He, C., Buonanno, G., McGarry, P., Maumy, B., Stabile, L., and Thai, P.K. (2019). Particle emissions from laser printers: have they decreased? *Environ. Sci. Technol. Lett.* *6*, 300–305.
54. Zhang, H., Yee, L.D., Lee, B.H., Curtis, M.P., Worton, D.R., Isaacman-VanWertz, G., Offenberg, J.H., Lewandowski, M., Kleindienst, T.E., Beaver, M.R., et al. (2018). Monoterpenes are the largest source of summertime organic aerosol in the southeastern United States. *Proc. Natl. Acad. Sci. USA* *115*, 2038–2043.
55. Park, J.H., Goldstein, A.H., Timkovsky, J., Fares, S., Weber, R., Karlik, J., and Holzinger, R. (2013). Active atmosphere-ecosystem exchange of the vast majority of detected volatile organic compounds. *Science* *341*, 643–647.
56. Bouvier-Brown, N.C., Schade, G.W., Misson, L., Lee, A., McKay, M., and Goldstein, A.H. (2012). Contributions of biogenic volatile organic compounds to net ecosystem carbon flux in a ponderosa pine plantation. *Atmos. Environ.* *60*, 527–533.
57. Holzinger, R., Lee, A., McKay, M., and Goldstein, A.H. (2006). Seasonal variability of monoterpene emission factors for a ponderosa pine plantation in California. *Atmos. Chem. Phys.* *6*, 1267–1274.
58. Mochizuki, T., Tani, A., Takahashi, Y., Saigusa, N., and Ueyama, M. (2014). Long-term measurement of terpenoid flux above a *Larix kaempferi* forest using a relaxed eddy accumulation method. *Atmos. Environ.* *83*, 53–61.
59. Tsui, J.K.-Y., Guenther, A., Yip, W.-K., and Chen, F. (2009). A biogenic volatile organic compound emission inventory for Hong Kong. *Atmos. Environ.* *43*, 6442–6448.
60. Zhou, M., Jiang, W., Gao, W., Zhou, B., and Liao, X. (2020). A high spatio-temporal resolution anthropogenic VOC emission inventory for Qingdao City in 2016 and its ozone formation potential analysis. *Process Saf. Environ. Prot.* *139*, 147–160.
61. Simayi, M., Shi, Y., Xi, Z., Li, J., Yu, X., Liu, H., Tan, Q., Song, D., Zeng, L., Lu, S., et al. (2020). Understanding the sources and spatiotemporal characteristics of VOCs in the Chengdu Plain, China, through measurement and emission inventory. *Sci. Total Environ.* *714*, 136692.
62. D'Angiola, A., Dawidowski, L.E., Gómez, D.R., and Osses, M. (2010). On-road traffic emissions in a megacity. *Atmos. Environ.* *44*, 483–493.
63. Kota, S.H., Park, C., Hale, M.C., Werner, N.D., Schade, G.W., and Ying, Q. (2014). Estimation of VOC emission factors from flux measurements using a receptor model and footprint analysis. *Atmos. Environ.* *82*, 24–35.
64. Karl, T., Striednig, M., Graus, M., Hammerle, A., and Wohlfahrt, G. (2018). Urban flux measurements reveal a large pool of oxygenated volatile organic compound emissions. *Proc. Natl. Acad. Sci. USA* *115*, 1186–1191.
65. Abbass, O.A., Sailor, D.J., and Gall, E.T. (2017). Effect of fiber material on ozone removal and carbonyl production from carpets. *Atmos. Environ.* *148*, 42–48.
66. Buhr, K., van Ruth, S., and Delahunty, C. (2002). Analysis of volatile flavour compounds by Proton Transfer Reaction-Mass Spectrometry: fragmentation patterns and discrimination between isobaric and isomeric compounds. *Int. J. Mass Spectrom.* *221*, 1–7.
67. de Lacy Costello, B., Amann, A., Al-Kateb, H., Flynn, C., Filipiak, W., Khalid, T., Osborne, D., and Ratcliffe, N.M. (2014). A review of the volatiles from the healthy human body. *J. Breath Res.* *8*, 014001.
68. Herbig, J., Müller, M., Schallhart, S., Titzmann, T., Graus, M., and Hansel, A. (2009). On-line breath analysis with PTR-TOF. *J. Breath Res.* *3*, 027004.
69. Mackay, D., Cowan-Ellsberry, C.E., Powell, D.E., Woodburn, K.B., Xu, S., Kozerski, G.E., and Kim, J. (2015). Decamethylcyclpentasiloxane (D5) environmental sources, fate, transport, and routes of exposure. *Environ. Toxicol. Chem.* *34*, 2689–2702.
70. Buser, A.M., Bogdal, C., MacLeod, M., and Scheringer, M. (2014). Emissions of decamethylcyclpentasiloxane from Chicago. *Chemosphere* *107*, 473–475.
71. Brown, S.K. (2002). Volatile organic pollutants in new and established buildings in Melbourne, Australia. *Indoor Air* *12*, 55–63.
72. Wang, C., Collins, D.B., Arata, C., Goldstein, A.H., Mattila, J.M., Farmer, D.K., Ampollini, L., DeCarlo, P.F., Novoselac, A., Vance, M.E., et al. (2020). Surface reservoirs dominate dynamic gas-surface partitioning of many indoor air constituents. *Sci. Adv.* *6*, eaay8973.
73. Algrim, L.B., Pagonis, D., de Gouw, J.A., Jimenez, J.L., and Ziemann, P.J. (2020). Measurements and modeling of absorptive partitioning of volatile organic compounds to painted surfaces. *Indoor Air* *30*, 745–756.
74. Weschler, C.J., and Nazaroff, W.W. (2008). Semivolatile organic compounds in indoor environments. *Atmos. Environ.* *42*, 9018–9040.
75. Elkilani, A.S., Baker, C.G.J., Al-Shammari, Q.H., and Bouhamra, W.S. (2003). Sorption of volatile organic compounds on typical carpet fibers. *Environ. Int.* *29*, 575–585.
76. Eichler, C.M.A., Cao, J., Isaacman-VanWertz, G., and Little, J.C. (2019). Modeling the formation and growth of organic films on indoor surfaces. *Indoor Air* *29*, 17–29.
77. Weschler, C.J., and Nazaroff, W.W. (2017). Growth of organic films on indoor surfaces. *Indoor Air* *27*, 1101–1112.
78. Liu, Q., and Abbatt, J.P.D. (2021). Liquid crystal display screens as a source for indoor volatile organic compounds. *Proc. Natl. Acad. Sci. USA* *118*, e2105067118.
79. Manninen, A.-M., Pasanen, P., and Holopainen, J.K. (2002). Comparing the VOC emissions between air-dried and heat-treated Scots pine wood. *Atmos. Environ.* *36*, 1763–1768.
80. Gall, E.T., Darling, E., Siegel, J.A., Morrison, G.C., and Corsi, R.L. (2013). Evaluation of three common green building materials for ozone removal, and primary and secondary emissions of aldehydes. *Atmos. Environ.* *77*, 910–918.
81. Tonidandel, S., and LeBreton, J.M. (2011). Relative importance analysis: A useful supplement to regression analysis. *J. Bus. Psychol.* *26*, 1–9.
82. Zhao, J., and Zhang, R. (2004). Proton transfer reaction rate constants between hydronium ion (H<sub>3</sub>O<sup>+</sup>) and volatile organic compounds. *Atmos. Environ.* *38*, 2177–2185.
83. Crilley, L.R., Lao, M., Salehpoor, L., and VandenBoer, T.C. (2023). Emerging investigator series: an instrument to measure and speciate the total reactive nitrogen budget indoors: description and field measurements. *Environ. Sci. Process Impacts* *25*, 389–404.
84. Yeung, L.L., and To, W.M. (2008). Size distributions of the aerosols emitted from commercial cooking processes. *Indoor Built Environ.* *17*, 220–229.

85. Xiong, J., He, Z., Tang, X., Misztal, P.K., and Goldstein, A.H. (2019). Modeling the time-dependent concentrations of primary and secondary reaction products of ozone with squalene in a university classroom. *Environ. Sci. Technol.* *53*, 8262–8270.
86. Fadeyi, M.O., Weschler, C.J., Tham, K.W., Wu, W.Y., and Sultan, Z.M. (2013). Impact of human presence on secondary organic aerosols derived from ozone-initiated chemistry in a simulated office environment. *Environ. Sci. Technol.* *47*, 3933–3941.
87. Tamas, G., Weschler, C.J., Bakobiro, Z., Wyon, D.P., and Stromtejsen, P. (2006). Factors affecting ozone removal rates in a simulated aircraft cabin environment. *Atmos. Environ.* *40*, 6122–6133.
88. Duncan, S.M., Tomaz, S., Morrison, G., Webb, M., Atkin, J., Surratt, J.D., and Turpin, B.J. (2019). Dynamics of Residential Water-Soluble Organic Gases: Insights into Sources and Sinks. *Environ. Sci. Technol.* *53*, 1812–1821.
89. Yang, S., Licina, D., Weschler, C.J., Wang, N., Zannoni, N., Li, M., Vanhanen, J., Langer, S., Wargocki, P., Williams, J., et al. (2021). Ozone initiates human-derived emission of nanocluster aerosols. *Environ. Sci. Technol.* *55*, 14536–14545.
90. Wagner, D.N., Mathur, A., and Boor, B.E. (2021). Spatial seated occupancy detection in offices with a chair-based temperature sensor array. *Build. Environ.* *187*, 107360.
91. Sadeghi, S.A., Karava, P., Konstantzos, I., and Tzempelikos, A. (2016). Occupant interactions with shading and lighting systems using different control interfaces: A pilot field study. *Build. Environ.* *97*, 177–195.
92. Lu, Y., Huang, J., Wagner, D.N., Lin, Z., Jung, N., and Boor, B.E. (2024). The influence of displacement ventilation on indoor carbon dioxide exposure and ventilation efficiency in a living laboratory open-plan office. *Build. Environ.* *256*, 111468.
93. Ding, X., Jiang, J., Tasoglou, A., Huber, H., Shah, A.D., and Jung, N. (2023). Evaluation of workplace exposures to volatile chemicals during COVID-19 building disinfection activities with proton transfer reaction mass spectrometry. *Ann. Work Expo Health* *67*, 546–551.
94. Jiang, J., Jung, N., and Boor, B.E. (2021). Using building energy and smart thermostat data to evaluate indoor ultrafine particle source and loss processes in a net-zero energy house. *ACS EST Eng.* *1*, 780–793.
95. Patra, S.S., Ramsisaria, R., Du, R., Wu, T., and Boor, B.E. (2021). A machine learning field calibration method for improving the performance of low-cost particle sensors. *Build. Environ.* *190*, 107457.